Chemical Vapor Deposition

DOI: 10.1002/cvde.200806756

Full Paper

Molecular Layer Deposition of Hybrid Organic-Inorganic Polymer Films using Diethylzinc and Ethylene Glycol**

By *Byunghoon Yoon*, *Jennifer L. O'Patchen*, *Dragos Seghete*, *Andrew S. Cavanagh*, and *Steven M. George**

The molecular layer deposition (MLD) of a hybrid organic-inorganic polymer based on zinc is demonstrated using sequential exposures of diethyl zinc (DEZ, $Zn(CH_2CH_3)_2$) and ethylene glycol (EG, $HOCH_2CH_2OH$). This polymer is representative of a class of zinc alkoxide polymers with an approximate formula of $(-Zn-O-R-O-)_n$ that can be called ''zincones''. The film growth and surface chemistry during zincone MLD is studied using in-situ Fourier transform infrared (FTIR) measurements. The absorbance of the infrared features of the zincone film increase progressively versus the number of MLD cycles. The FTIR spectra after the DEZ and EG exposures are consistent with the gain and loss of absorbance from C–H, O–H, C–O, and Zn–O stretching vibrations. FTIR studies also confirm the self-limiting nature of the surface reactions and monitor the temperature dependence of the film growth. Transmission electron microscope (TEM) images of ZrO_2 nanoparticles show very conformal zincone films and determine that the growth rate varies from 4.0 Å per MLD cycle at 90 °C to 0.25 Å per MLD cycle at 170 °C. Quartz crystal microbalance (QCM) and X-ray reflectivity (XRR) measurements show linear zincone growth versus the number of MLD cycles. XRR studies on silicon wafers are consistent with a growth rate of 0.7 Å per MLD cycle at 130 °C. The higher growth rate on the ZrO_2 nanoparticles is attributed to the lower gas conductance and possible CVD reactions in the ZrO_2 nanoparticles. The reaction mechanism for zincone MLD is dependent on temperature. At higher temperatures, there is evidence for ''double'' reactions of EG because no free hydroxyl groups are observed in the FTIR spectrum after the EG exposures. The zincone film can grow in the absence of free hydroxyl groups if DEZ can diffuse into the zincone film and react during the subsequent EG exposure. The zincone films initially adsorb H_2O upon exposure to air and then are very stable with time.

Keywords: Hybrid organic-inorganic materials, Molecular layer deposition, Polymer films, Surface chemistry

1. Introduction

Molecular layer deposition (MLD) is based on sequential and self-limiting surface reactions of reactants containing organic constituents.[1,2] MLD methods are very similar to atomic layer deposition (ALD) techniques that have been developed for the growth of inorganic materials.[3–5] Both MLD and ALD can be used to fabricate conformal, continuous, and pinhole-free films.[6–9] The self-limiting nature of the surface chemistry allows conformal MLD and ALD films to be grown on high aspect ratio and porous structures.[10]

Recent work has demonstrated the MLD of organic polymer films using homobifunctional reactants. For example, polyamide films such as Nylon 66 have been deposited using adipoyl chloride and 1,6–hexanediamine as the reactants.[11] Poly(*p*–phenylene terephthalamide) films have also been grown using terephthaloyl chloride and *p*–phenylenediamine as the reactants.[12] The MLD of organic polyimide films has also been reported using diamines and carboxylic anhydrides.[13] Earlier work also demonstrated the MLD of polyimides,[2,14] polyamides,[15] and polyureas.[16] In some of the these earlier studies, the method of sequential, self-limiting surface reactions was known as alternating vapor deposition polymerization.[15,17]

In addition to the MLD of organic polymers, the MLD of hybrid organic-inorganic polymer films was recently accomplished using trimethyl aluminum (TMA, $Al(CH_3)_3$) and EG.[6] These organic-inorganic composite films combine an

[*] Prof. S. M. George, Dr. B. Yoon, J. L. O'Patchen, D. Seghete
Department of Chemistry and Biochemistry, University of Colorado
Boulder, CO 80309-0215 (USA)
E-mail: Steven.George@Colorado.edu
A. S. Cavanagh
Department of Physics, University of Colorado
Boulder, CO 80309-0215 (USA)
Prof. S. M. George, A. S. Cavanagh
DARPA Center for Integrated Micro/Nano-Electromechanical Transducers (iMINT), University of Colorado
Boulder, CO 80309-0215 (USA)
Prof. S. M. George
Department of Chemical and Biological Engineering,
University of Colorado
Boulder, CO 80309-0215 (USA)

[**] This work was supported by the National Science Foundation (CHE-0715552). Some of the equipment used in this research was provided by the Air Force Office of Scientific Research. DS was supported by DARPA/MTO, SPAWAR (Contract No. N66001-07-1-2033). ASC was supported by the DARPA Center on NanoscaleScience and Technology for Integrated Micro/Nano-Electromechanical Transducers (iMINT) funded by DARPA N/MEMS S&T Fundamentals Program (HR0011-06-1-0048).

Report Documentation Page

Form Approved
OMB No. 0704-0188

1. REPORT DATE	2. REPORT TYPE	3. DATES COVERED
2009		**00-00-2009 to 00-00-2009**

4. TITLE AND SUBTITLE	5a. CONTRACT NUMBER
Molecular Layer Deposition of Hybrid Organic-Inorganic Polymer Films using Diethylzinc and Ethylene Glycol	5b. GRANT NUMBER
	5c. PROGRAM ELEMENT NUMBER
6. AUTHOR(S)	5d. PROJECT NUMBER
	5e. TASK NUMBER
	5f. WORK UNIT NUMBER
7. PERFORMING ORGANIZATION NAME(S) AND ADDRESS(ES) **University of Colorado,Department of Chemistry and Biochemistry,Boulder,CO,80309**	8. PERFORMING ORGANIZATION REPORT NUMBER
9. SPONSORING/MONITORING AGENCY NAME(S) AND ADDRESS(ES)	10. SPONSOR/MONITOR'S ACRONYM(S)
	11. SPONSOR/MONITOR'S REPORT NUMBER(S)

12. DISTRIBUTION/AVAILABILITY STATEMENT
Approved for public release; distribution unlimited

13. SUPPLEMENTARY NOTES

14. ABSTRACT

15. SUBJECT TERMS

16. SECURITY CLASSIFICATION OF:			17. LIMITATION OF ABSTRACT	18. NUMBER OF PAGES	19a. NAME OF RESPONSIBLE PERSON
a. REPORT **unclassified**	b. ABSTRACT **unclassified**	c. THIS PAGE **unclassified**	**Same as Report (SAR)**	**10**	

inorganic reactant, TMA, with an organic reactant, EG. The general family of organic-inorganic polymers with the approximate form of $(-Al-O-R-O-)_n$ are known as ''alucones''.[6,18] The reaction of TMA and EG is one of a large number of reactions between metal alkyls and organic diols. The metal alkyl molecule can be described by MR_x and the diol can be described by HOR'OH. The general MLD reactions between the metal alkyl and the diol can be written as Equations 1 and 2.[6]

$$(A)\ ROH* + MR'_x \rightarrow RO - MR'^{*}_{x-1} + R'H \quad (1)$$

$$(B)\ MR'^{*} + HOROH \rightarrow M - OROH^{*} + R'H \quad (2)$$

The asterisks indicate the surface species. These A and B reactions in an ABAB... sequence of metal alkyl and organic diol can lead to the growth of the hybrid organic-inorganic polymeric films.

Many metal alkyls and organic reactants can be used to define various hybrid organic-inorganic MLD polymers.[1] For example, zinc alkyls such as $Zn(CH_2CH_3)_2$ (diethyl zinc (DEZ)) and $TiCl_4$ (titanium tetrachloride) should react with diols in a similar MLD process. Other metal alkyls that can easily react with oxygen precursors are also candidates for hybrid organic-inorganic polymer MLD. Examples include metal alkyls based on magnesium (Mg) and manganese (Mn), such as $Mg(C_p)_2$ and $Mn(C_p)_2$ where C_p is the cyclopentadienyl ligand, that react readily with H_2O.[19,20] In addition, many other oxygen-containing bifunctional organic reactants are possible such as carboxylic acids and aldehydes.[21] Homobifunctional organic reactants such as diamines or dithiols should also be possible precursors.

In this paper, the MLD of a hybrid organic-inorganic polymer based on zinc was demonstrated using DEZ and EG as the reactants.[22,23] These zinc-containing polymer films are part of a class of zinc alkoxide polymers with a composition approximated by $(-Zn-O-R-O-)_n$. This class of zinc alkoxide films can be called ''zincones'' in analogy with the closely-related alucones.[6,18] The proposed surface reactions for zincone MLD using DEZ and EG are expected to follow the chemical reactions described by Equations 1 and 2. A schematic depicting the zincone MLD growth is shown in Figure 1.

The overall zincone MLD reaction using DEZ and EG can be written as Equation 3.

$$n Zn(CH_2CH_3)_2 + n HOCH_2CH_2OH \rightarrow (-Zn-O-CH_2CH_2-O-)_n + n CH_3CH_3 \quad (3)$$

The reaction of DEZ and EG is analogous to the reaction of $DEZ + H_2O \rightarrow ZnO + 2C_2H_6$ for ZnO ALD.[24–26] This reaction has favorable thermochemistry with an enthalpy of reaction of $\Delta H = -70.0$ kcal.[27] The DEZ + EG reaction is expected to have a very similar enthalpy of reaction because the same bonds are broken and formed during the DEZ + EG and DEZ + H_2O reactions. There is also precedence for the DEZ + EG MLD reaction. Polymerization reactions using organic diols and dialkylzinc precursors have been studied in organic solution under an argon environment.[28]

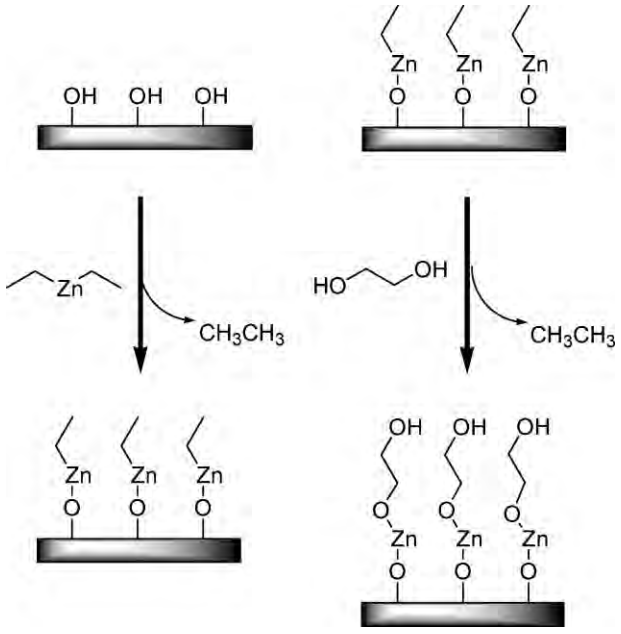

Fig. 1. Schematic for growth mechanism of zincone MLD film using DEZ and EG.

This investigation of zincone MLD concentrated on in-situ FTIR spectroscopy to monitor the zincone MLD growth, to identify the surface species following the DEZ and EG reactions, and to verify the self-limiting nature of the surface reactions. XRR studies measured the thickness of the zincone films and the linearity of zincone MLD growth versus number of MLD cycles. TEM was used to image the zincone films on ZrO_2 nanoparticles and obtain the temperature dependence of the zincone MLD growth. In-situ QCM measurements were used to verify the linearity of zincone MLD. X-ray photoelectron spectroscopy (XPS) was employed to characterize the elemental composition of the zincone films. These studies help to establish the generality and feasibility of MLD reactions based on metal alkyls and organic diols.

2. Results and Discussion

2.1. Zincone MLD Growth

Zincone MLD was studied using in-situ FTIR studies over the temperature range 90–170 °C. FTIR spectra were recorded after various numbers of MLD cycles and after each reactant exposure. The FTIR spectra after various numbers of MLD cycles monitor the progressive growth of

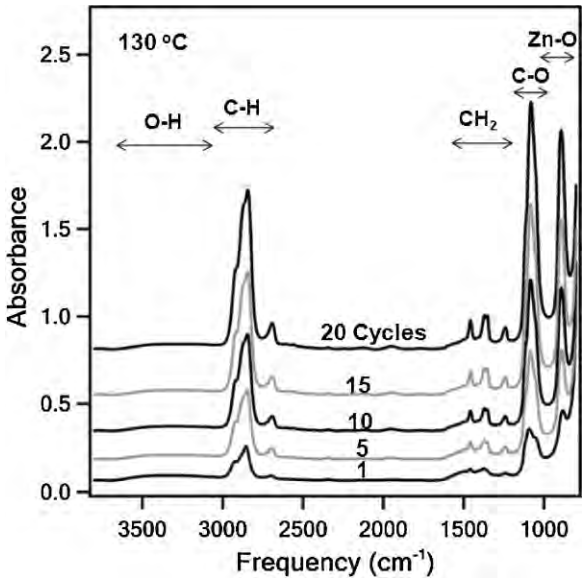

Fig. 2. In-situ FTIR spectra during the growth of zincone MLD films after 1, 5, 10, 15, and 20 MLD cycles at 130 °C.

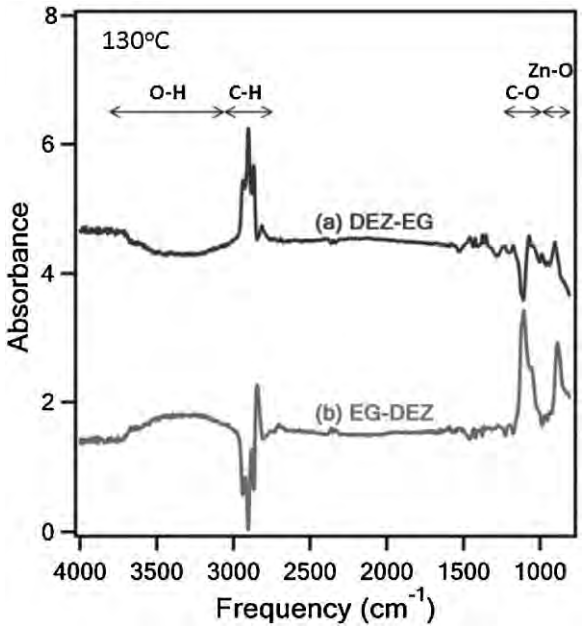

Fig. 3. FTIR difference spectra after DEZ and EG exposures during zincone MLD film growth at 130 °C. a) DEZ-EG after DEZ exposure on a film previously reacted with EG. b) EG-DEZ after EG exposure on a film previously reacted with DEZ.

the zincone film. Figure 2 displays the FTIR spectra following the EG exposures after 1, 5, 10, 15, and 20 MLD cycles at 130 °C. The infrared absorbance grows progressively with number of MLD cycles.

Prominent absorbances are observed in Figure 2 at 2800–3000 cm^{-1} corresponding to the C–H stretching vibrations of the ethylene linkages between oxygen atoms in the zinc alkoxide polymer. At lower frequencies, large absorbance is also observed at 888 cm^{-1} and 1100 cm^{-1}. These absorbances are assigned to Zn–O and C–O stretching vibrations. Smaller absorbances at 1456 cm^{-1}, 1365 cm^{-1}, and 1256 cm^{-1} are also monitored in Figure 2 and assigned to CH_2 scissors, wag, and twist modes, respectively. These vibrational features are all consistent with the growth of a zinc alkoxide polymer that may be approximated by $(-Zn-O-CH_2CH_2-O-)_n$. There is also a weak and broad absorbance at 3100–3730 cm^{-1} assigned to O–H stretching vibrations. This vibrational feature is observed after the EG exposures.

The change in surface species during each reaction can be monitored by the FTIR difference spectra. The surface species that are added appear as positive absorbance features and the surface species that are removed appear as negative absorbance features. The FTIR difference spectra for the DEZ exposure referenced against the EG exposure (DEZ-EG) and the EG exposure referenced against the DEZ exposure (EG-DEZ) at 130 °C are shown in Figures 3a and 3b, respectively.

In the difference spectrum for DEZ-EG in Figure 3a, the positive features are the absorbances of the CH_2 and CH_3 stretching vibrations for the ethyl group of the DEZ surface species at 2910 and 2941 cm^{-1}. The gain of these C–H stretching vibrations from the ethyl group is very similar to previous studies that explored DEZ reactions on ZrO_2 and $BaTiO_3$ surfaces.[25] A negative absorbance feature is observed in Figure 3a at 3100–3730 cm^{-1}. This feature is consistent with the removal of hydroxyl species. There is also evidence for a slight frequency shift and reduction of the absorbance at 1100 cm^{-1} corresponding to the C–O stretching vibration.

In the difference spectrum for EG-DEZ in Figure 3b, the spectrum appears as the inverse of the DEZ-EG spectrum in the O–H and C–H stretching region. The positive absorbance features are observed for the O–H, C–O, and Zn–O stretching vibrations at 3100–3730 cm^{-1}, 1100 cm^{-1}, and 888 cm^{-1}, respectively. There are also positive absorbance features for the CH_2 symmetric and asymmetric stretching vibrations at 2850 and 2885 cm^{-1}. The negative features are the absorbances for the CH_2 and CH_3 stretching vibrations for the ethyl group of the DEZ surface species at 2910 and 2941 cm^{-1}. The gain and loss of CH_2 and CH_3 features leads to a complicated spectrum in the C–H stretching vibration region.

The integrated absorbance of the C–H stretching vibrations at 2800–3000 cm^{-1} and the integrated absorbance of the O–H stretching vibrations at 3100–3730 cm^{-1} can be used to monitor the self-limiting nature of the DEZ and EG reactions. The integrated absorbance for the C–H stretching vibrations versus DEZ exposure at 130 °C is shown in Figure 4a. The integrated absorbance for the O–H stretching vibrations versus EG exposure at 130 °C is shown in Figure 4b. In both cases, the exposures are defined by the number of microdoses of DEZ or EG. Figure 4a indicates that the DEZ reaction is self-limiting and reaches

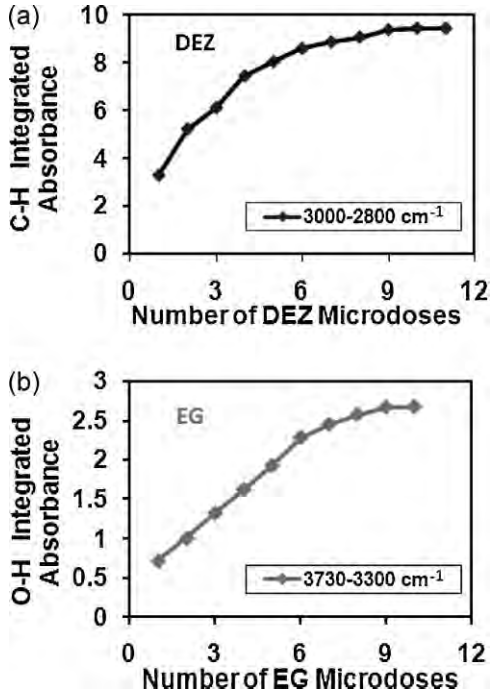

Fig. 4. Integrated absorbance for a) C–H stretching vibrations versus number of DEZ microdoses, and b) O–H stretching vibrations versus number of EG microdoses. Both DEZ and EG exposures were performed at 130 °C.

completion after ten DEZ microdoses. Each DEZ dose was defined by a 0.3 s exposure at 70 mTorr of partial pressure. Likewise, Figure 4b indicates that the EG reaction also is self-limiting and reaches completion after 10 EG microdoses. Each EG dose was defined by a 0.3 s exposure at 8–10 mTorr of partial pressure.

2.2. Assignment of Vibrational Features

The assignments of the vibrational frequencies observed during zincone MLD growth are given in Table 1. Most of these vibrational features have been identified previously.[29] The Zn–O stretching vibration was assigned to the absorbance feature at 888 cm^{-1}. In contrast, a recent FTIR study of the reaction of DEZ with alcohols observed a vibrational feature at 755 cm^{-1} that was tentatively assigned to the Zn–O stretching vibration.[30] Other studies on ZnO nanoparticles have observed features at 400–600 cm^{-1} that have been associated with Zn–O vibrations.[31] Additional investigations of the metal-organic vapor pressure epitaxy growth of ZnO with DEZ and N_2O have observed a broad infrared feature at 760–950 cm^{-1}.[32] This infrared peak was believed to correspond with various polymer fragments resulting from $C_2H_5OZnC_2H_5$, $Zn(OC_2H_5)_2$, $HOZnOC_2H_5$, and $Zn(OH)_2$ reaction products that oligomerize by forming Zn–O bonds.[32]

Table 1. Assignment of vibrational peaks observed during zincone MLD.

Frequency [cm^{-1}]	Assignment
3730	O–H stretch, EG
2941	CH_3 asymmetric stretch, DEZ
2910	CH_2 asymmetric stretch, DEZ
2885	CH_2 asymmetric stretch, EG
2871	CH_2 stretch, DEZ
2850	CH_2 symmetric stretch, EG
2787	CH_2 stretch, DEZ
2697	EG combination
1456	CH_2 scissors
1365	CH_2 wag
1256	CH_2 twist
1100	C–O stretch
888	Zn–O stretch, EG and DEZ

To confirm that there are no Zn–O stretching vibrations at frequencies lower than 888 cm^{-1} that may be obscured by absorption from ZrO_2 nanoparticles, zincone MLD was performed on SiO_2 nanoparticles. In these studies, no new vibrational features were observed in the EG-DEZ difference spectrum between 600–850 cm^{-1}. The absence of vibrational features at lower frequencies helps to confirm that the vibrational feature at 888 cm^{-1} is characteristic for the Zn–O stretching vibration in the zincone films.

Another vibrational feature was observed with a peak at ~1590 cm^{-1} when the EG was exposed in a static mode with the gate valve closed to the pumps. This feature was accompanied by an increased absorbance in the O–H stretching region at ~3000–3680 cm^{-1}. These two features are consistent with the absorption of H_2O molecules on the surface of the zincone film. H_2O may be an impurity in EG and is a decomposition product of EG.[33] These features at ~1590 cm^{-1} and ~3000–3680 cm^{-1} observed after static EG exposures suggest that zincone MLD growth may be strongly affected by pumping speed and purging times. We note that the feature at ~1590 cm^{-1} was also observed when the liquid N_2 trap was not pumping on the reactor.

2.3. Temperature Dependence of Zincone MLD

The integrated absorbance of the C–H stretching vibrations can be used to determine the temperature dependence of zincone MLD. For these experiments, the absorbance in the C–H stretching region was measured after ten zincone MLD cycles at various temperatures in the range 90–170 °C. These FTIR spectra in the C–H stretching region are shown in Figure 5. After ten MLD cycles, the absorbance in the C–H stretching region decreases progressively for zincone MLD at higher temperatures. This decrease in the zincone MLD growth per cycle at higher temperatures is consistent with previous results for alucone MLD.[6]

The temperature dependence of the zincone MLD growth per cycle was also measured using TEM analysis of zincone films grown on ZrO_2 nanoparticles at various temperatures. The TEM image of a zincone film after thirty MLD cycles at 130 °C is shown in Figure 6. This TEM image reveals that the

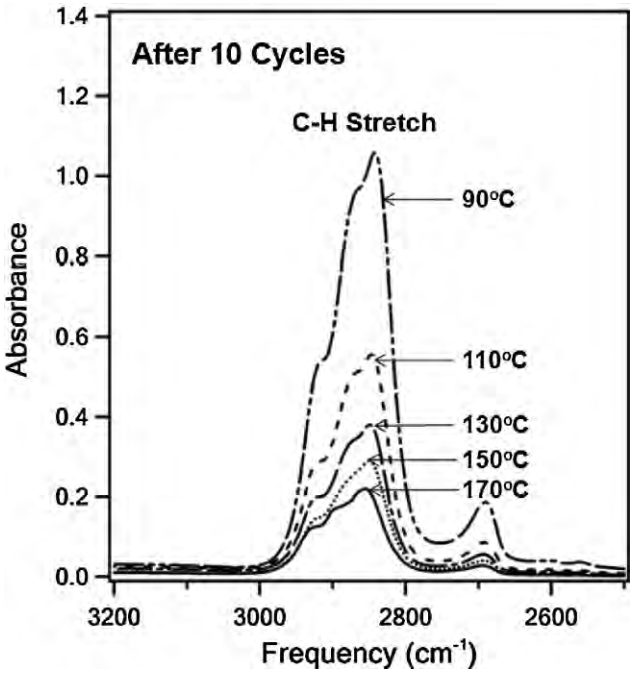

Fig. 5. FTIR vibrational spectra for absorbance in the C–H stretching vibration region after 10 MLD cycles at 90, 110, 130, 150, and 170 °C.

zincone film is very conformal on the ZrO_2 nanoparticles. The thickness of 61 Å after thirty MLD cycles at 130 °C is consistent with a zincone MLD growth rate of 2.0 Å per MLD cycle. Thirty cycles of zincone MLD was repeated on ZrO_2 nanoparticles at various temperatures in the range 90–170 °C. The TEM images were consistent with a zincone MLD growth rate that was 4.0 Å per MLD cycle at 90 °C, and reduced to 0.25 Å per MLD cycle at 170 °C.

Figure 7 displays the zincone MLD growth per cycle versus temperature determined by the TEM analysis. These results are compared with the integrated absorbance for the C–H stretching vibrations of zincone films after ten MLD cycles at various temperatures. The integrated absorbance has been scaled to match the growth per cycle determined by the TEM measurements. The temperature-dependent

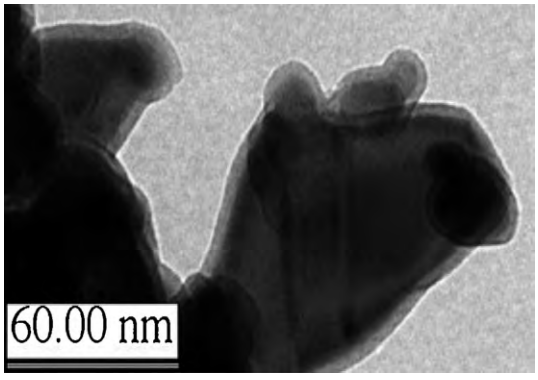

Fig. 6. TEM image of zincone MLD film on ZrO_2 nanoparticles after 30 MLD cycles at 130 °C.

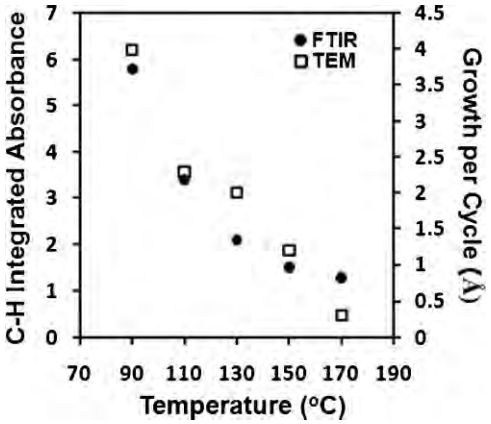

Fig. 7. Comparison between the integrated absorbance for the C–H stretching vibrations in Fig. 5 after 10 MLD cycles and the growth per cycle for zincone MLD measured by TEM analysis of ZrO_2 nanoparticles at 90, 110, 130, 150, and 170 °C.

results from the TEM and integrated absorbance analysis are in excellent agreement.

The decrease in the zincone MLD growth per cycle versus temperature can be partly attributed to the diffusion of DEZ into the zincone film. Similar to alucone MLD,[6] the zincone film growth is believed to occur by both the surface chemistry, described by Equations 1 and 2, and the diffusion of DEZ into the zincone film. The DEZ molecules that diffuse into the MLD film are available to react during the subsequent EG exposure to form new zincone polymer chains. This additional growth mechanism is similar to a CVD reaction in the near-surface region of the zincone polymer. This diffusion mechanism can explain the temperature dependence of the zincone MLD growth. At higher temperatures, less DEZ may diffuse into the zincone film. In addition, the DEZ in the zincone film may desorb

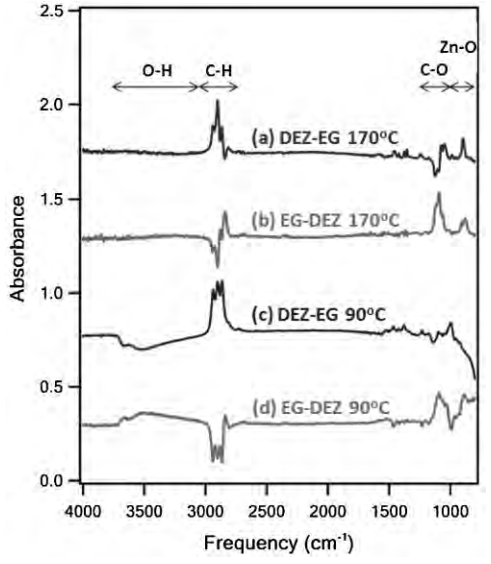

Fig. 8. FTIR difference spectra for a) DEZ-EG at 170 °C, b) EG-DEZ at 170 °C, c) DEZ-EG at 90 °C, and d) EG-DEZ at 90 °C.

from the film at a faster rate at higher temperatures. Less diffusion into the film and more desorption of DEZ from the film would yield a lower zincone MLD growth per cycle at higher temperatures.

In addition to lower growth per cycle for zincone MLD at higher temperatures, the mechanism of zincone MLD also changes with temperature. Figure 8 compares FTIR difference spectra for DEZ-EG and EG-DEZ at 90 °C and 170 °C. For growth at 170 °C, there is negligible absorbance change in the O–H stretching vibration region in Figure 8a for DEZ-EG or Figure 8b for EG-DEZ. The absence of hydroxyl groups either removed by DEZ or produced by EG suggests that most of the EG reactions are ''double'' reactions at 170 °C. If EG reacts with two $ZnCH_2CH_3^*$ species, then there are no new O–H stretching vibrations after the EG exposure.

Although there is negligible absorbance change for O–H stretching vibrations shown in Figure 8a, there is an increase in absorbance for C–H stretching vibrations of the $ZnCH_2CH_3^*$ species after DEZ exposures. This absorbance increase is consistent with the diffusion of DEZ into the zincone film at 170 °C. Figure 8a also shows that the DEZ exposure produces very little increase in the absorbance for the C–O and Zn–O stretching vibrations that would be consistent with $-ZnOCH_2CH_2OZn-$ species. This observation argues that the DEZ diffuses into the zincone film without reacting with hydroxyl groups.

Figure 8b shows that the EG exposure at 170 °C removes absorbance for the C–H stretching vibrations from $ZnCH_2CH_3^*$ and adds absorbance for the C–H stretching vibrations from $-OCH_2CH_2O-$ species. There are also increases in the absorbance of the C–O and Zn–O stretching vibrations. These absorbance changes, together with the absence of absorbance changes for the O–H stretching vibrations, are consistent with the reaction of EG with two $ZnCH_2CH_3^*$ species to form $-ZnOCH_2CH_2OZn-$ at 170 °C. The ''double'' reactions of EG remove $ZnCH_2CH_3^*$ sites and do not generate $ZnOCH_2CH_2OH^*$ hydroxyl sites for zincone film growth. However, a finite amount of DEZ diffusion into the zincone film during DEZ exposure maintains the low zincone growth rate of ~0.25 Å per MLD cycle at 170 °C.

Much larger growth rates of ~4.0 Å per cycle are observed at the low temperature of 90 °C. Figures 8c and 8d reveal that hydroxyl groups are active during zincone MLD at 90 °C. Figure 8c shows that there is a decrease in absorbance for O–H stretching vibrations after the DEZ exposure. Likewise, Figure 8d reveals a gain in absorbance for O–H stretching vibrations after the EG exposure. There still may be double reactions during the EG exposure. However there are also EG reactions that produce hydroxyl groups on the zincone film.

The spectrum for DEZ-EG in Figure 8c reveals that there is a large absorbance increase in the C–H stretching region for the $ZnCH_2CH_3^*$ species. The correspondingly low increase of absorbance for C–O and Zn–O stretching vibrations suggests that much of the DEZ is diffusing into the zincone polymer without reacting with hydroxyl groups at 90 °C. The spectrum for EG-DEZ in Figure 8d shows a loss of absorbance from C–H stretching vibrations of the $ZnCH_2CH_3^*$ species, and a gain of absorbance from C–O and Zn–O stretching vibrations. These absorbance changes, together with the presence of absorbance changes for the O–H stretching vibrations, are consistent with the reaction between EG and $ZnCH_2CH_3^*$ species to form both $ZnOCH_2CH_2OH^*$ and $-ZnOCH_2CH_2OZn-$ species at 90 °C.

2.4. Linear Zincone MLD Growth

The quality and thickness of zincone films grown on Si wafers at 130 °C was also measured using ex-situ XRR analysis. The XRR scans were fitted using the REFS data fitting software from Bede Scientific. For this XRR analysis, an Al_2O_3 ALD film with a thickness of ~640 Å was initially deposited on the silicon wafer using TMA and H_2O. Subsequently, zincone films were grown on the Al_2O_3 ALD layer. Figure 9a shows the XRR scan, approximately one hour after deposition, of a zincone film grown using 500 MLD cycles at 130 °C. This scan displays an oscillatory reflected intensity versus angle. The oscillation occurs as the intensity drops over many orders of magnitude. This behavior is consistent with a very smooth and high quality film. The oscillatory intensity results from the film thickness and the individual Al_2O_3 and zincone layers. Figure 9b displays the XRR scan of the same film after five weeks in air. The XRR scans in Figures 9a and 9b are nearly identical, and indicate that the zincone film is very stable.

Figure 10a shows the zincone film thicknesses measured by XRR after 80, 150, and 500 MLD cycles at 130 °C. The film thickness versus number of MLD cycles is linear and consistent with a growth rate of 0.7 Å per MLD cycle at 130 °C. The growth rate of 0.7 Å per MLD cycle at 130 °C on the silicon wafer is less than the growth rate of 2.0 Å per

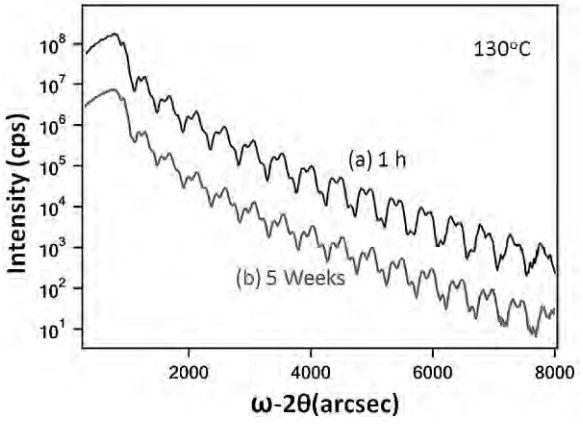

Fig. 9. XRR scans of zincone film grown on Si wafer using 500 MLD cycles at 130 °C after a) ~1 h exposure in air, and b) ~5 weeks exposure in air.

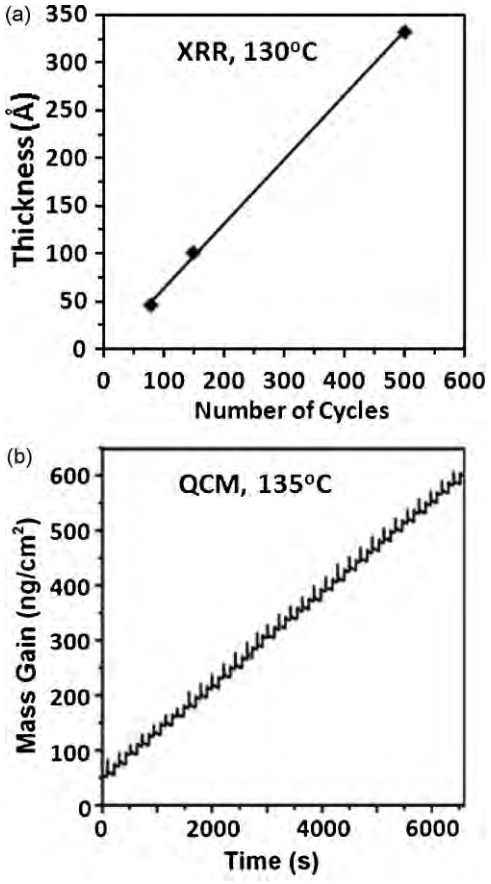

Fig. 10. a) XRR measurements of zincone film thickness versus number of MLD cycles at 130 °C. b) QCM measurements of mass gain versus time for zincone MLD film growth at 135 °C.

MLD cycle at 130 °C on the ZrO_2 nanoparticles. The different growth rates on the Si wafer and the ZrO_2 nanoparticles can be explained by either different pumping speeds during the zincone MLD growth experiments, or the low gas conductance in the ZrO_2 nanoparticles. In the ZrO_2 nanoparticles, longer exposure times are needed for the reactants to reach the entire surface area. In addition, longer purge times are needed to remove the reactants after their exposure. If the reactant is not completely purged from the bed of nanoparticles, then the zincone MLD growth rate can increase resulting from CVD growth.

In-situ QCM measurements also revealed that the zincone MLD growth was linear versus the number of MLD cycles. Typical results from the QCM analysis of zincone MLD at 135 °C are shown in Figure 10b. The reactant pulse sequence during one MLD cycle was; DEZ dose for 0.75 s, purge for 120 s, EG dose for 0.45 s, and purge for 120 s. These dose times resulted in approximate exposures of 65 mTorr s for DEZ and 80 mTorr s for EG. The mass gain per MLD cycle was 20.4 ng cm^{-2} for the QCM results at 135 °C shown in Figure 10b. The QCM measurements also demonstrated that the DEZ and EG reactions were self-limiting. The mass gains reached an asymptotic limit versus DEZ and EG exposures. Although the zincone MLD growth was linear versus number of MLD cycles under one set of reaction conditions, the absolute mass gain per cycle and the mass gains for the individual DEZ and EG reactions during one cycle were not consistent for experiments on different days. This inconsistency is believed to result from the variations in the pumping speed during different zincone MLD growth experiments.

2.5. Composition and Stability of Zincone Films

The composition of the zincone films was investigated using XPS. Figure 11 shows XPS results for a zincone film grown using 500 MLD cycles at 130 °C. The average composition obtained from several such films was 10% zinc, 22% carbon, and 68% oxygen. The uncertainty on these at.-% values is <2%. These atomic percentages are based on peak areas of each component. The adventitious carbon at 285 eV was not included in this XPS analysis. No other elements are present in the zincone film. In contrast, a composition can be predicted (20% zinc, 40% carbon, and 40% oxygen) for the zincone film based on the reaction mechanism shown in Figure 1, and a possible polymer formula of $(-Zn-O-CH_2CH_2-O-)_n$. The zincone film has less zinc and more oxygen than predicted by the expected formula. The higher oxygen and lower zinc atomic percentages are related to the adsorption of H_2O into the zincone films upon exposure to air. As discussed earlier in Section 2.2, the in-situ FTIR spectra during static EG exposures were consistent with H_2O adsorption. Features assigned to H_2O adsorption at ~1590 cm^{-1} were also present when the liquid N_2 trap was not used to pump on the reactor.

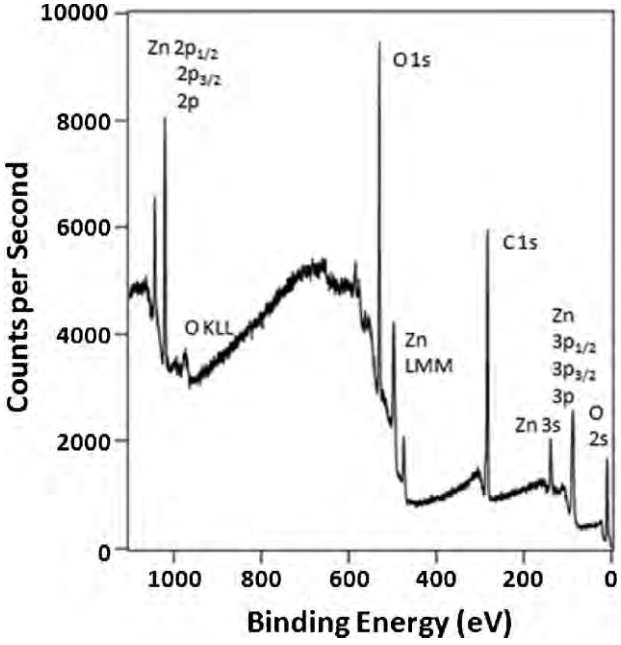

Fig. 11. XPS analysis of zincone MLD film composition after 500 MLD cycles at 130 °C.

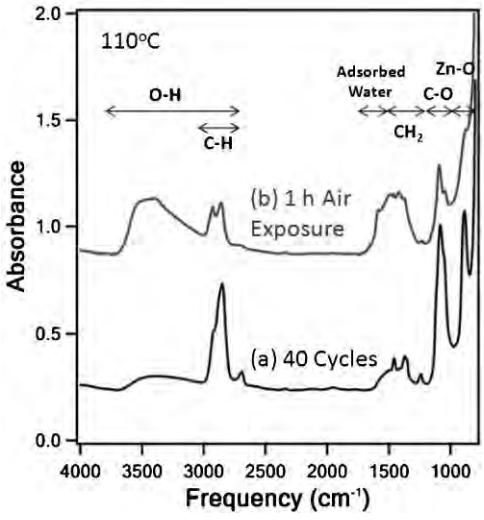

Fig. 12. a) Absolute in-situ FTIR spectrum of zincone film grown using 40 MLD cycles at 110 °C. This spectrum was recorded with the zincone film under vacuum in the MLD reactor. b) Absolute FTIR spectrum of the same film after ~1 h exposure in air.

There was also evidence from the FTIR spectra for H_2O adsorption into the zincone films after exposing the zincone films to air.

Figure 12a shows the absolute in-situ FTIR spectrum of a zincone film deposited after 40 MLD cycles at 110 °C. This spectrum was recorded with the zincone film under vacuum in the MLD reactor. Figure 12b displays the absolute FTIR spectrum of the same zincone film after approximately one hour of air exposure. This spectrum reveals the growth of absorbance corresponding with O–H stretching vibrations in the range 2700–3700 cm^{-1}. There are also adsorbed H_2O modes and broadened CH_2 features in the range 1300–1700 cm^{-1}.[34] Very little subsequent change was observed after weeks of air exposure. These FTIR results indicate that the zincone films adsorb H_2O upon exposure to air. However, the FTIR and XRR results reveal that the zincone films are very stable following this initial H_2O adsorption.

After the initial adsorption of H_2O upon exposure to air, the zincone MLD films are more stable than the alucone MLD films studied previously.[6] The stability of the zincone films was confirmed by the XRR measurements at various times after film growth shown in Figure 9. These XRR scans revealed almost no change in the thickness of the zincone films after aging for weeks at room temperature under ambient air conditions. For example, for a zincone film with a thickness of ~335 Å grown using 500 MLD cycles at 130 °C, the thickness decreased only 2.4% after aging for five weeks. In contrast, the alucone MLD film thicknesses decreased about 22% in the first six days after growth at room temperature under ambient air conditions.[6]

The zinc composition was also investigated after growth at various temperatures. XPS measurements on zincone MLD samples grown using 80 MLD cycles at 90, 110, 130, 150, and 170 °C yielded zinc compositions of 10.7, 10.6, 10.0. 9.9, and 8.9%, respectively. These XPS results indicate that the zinc atomic percentages are very consistent over the full range of temperatures. The changes in the zincone MLD growth mechanism and the observation of only double EG reactions at higher temperatures do not alter the zincone film composition.

3. Conclusions

The MLD of a new zinc-containing organic-inorganic polymer was grown using the sequential exposures of DEZ and EG. This polymer represents a new type of zinc alkoxide polymers that can be called zincones. The MLD procedure used to grow the zincone film is similar to the sequential exposures of TMA and EG used for alucone MLD. This work indicates that a variety of different hybrid organic-inorganic polymers can be grown by MLD using metal alkyl precursors and various organic precursors.

The film growth and surface chemistry during zincone MLD was studied by in-situ FTIR measurements. The FTIR spectra increased progressively versus the number of MLD cycles. FTIR spectra after the EG and DEZ exposures were consistent with loss and gain of the absorbance for C–H, O–H, C–O, and Zn–O stretching vibrations. FTIR studies also confirmed the self-limiting nature of the surface reactions and monitored lower zincone MLD growth rates at higher temperatures.

TEM measurements on ZrO_2 nanoparticles observed very conformal zincone films. The TEM studies also determined that the zincone MLD growth rate varied from 4.0 Å per MLD cycle at 90 °C to 0.25 Å per MLD cycle at 170 °C. XRR measurements on silicon wafers displayed linear zincone MLD growth with a lower zincone MLD growth rate of 0.7 Å per MLD cycle at 130 °C. Different pumping speeds, lower gas conductance, and possible CVD reactions may explain the higher zincone MLD growth rates on the ZrO_2 nanoparticles. QCM measurements confirmed linear growth for the zincone films versus the number of MLD cycles.

The FTIR difference spectra indicated that the reaction mechanism for zincone MLD was dependent on temperature. At higher temperatures, no free hydroxyl groups were present in the zincone film as demonstrated by the absence of O–H stretching vibrations in the FTIR spectra. The absence of free hydroxyl species may be explained by a double reaction of EG with two $ZnCH_2CH_3^*$ species. The lack of hydroxyl groups does not stop the zincone MLD film growth at higher temperatures. The FTIR spectra suggested that DEZ can diffuse into the zincone film and nucleate the growth of a new zincone polymer chain.

The zincone MLD films were observed to adsorb H_2O after exposure to air. This H_2O adsorption is monitored by the FTIR spectra and is consistent with the high oxygen and low zinc composition in the zincone films obtained by XPS analysis. Following the H_2O adsorption, the zincone films are very stable for multiple weeks as determined by FTIR

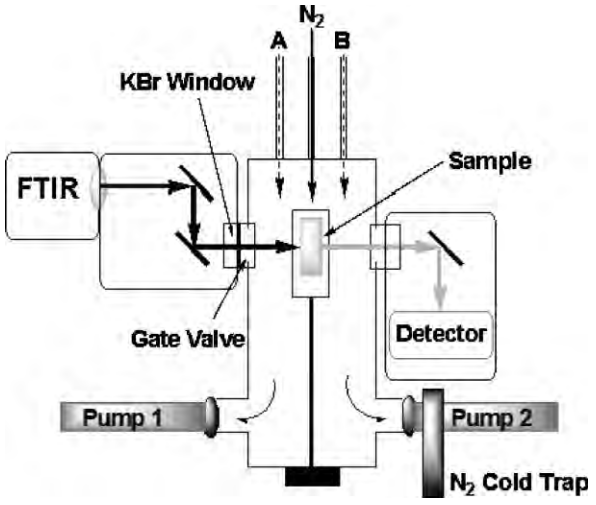

Fig. 13. Schematic diagram of viscous flow MLD reactor equipped with in-situ FTIR spectrometer.

and XRR measurements. These new zincone films add to the growing list of possible MLD thin films. The zincone films may have many interesting applications because of their hybrid organic-inorganic properties.

4. Experimental

A schematic diagram of the viscous flow MLD reactor equipped with an in-situ FTIR spectrometer is shown in Figure 13. This viscous flow MLD reactor is very similar to previous reactors used for MLD [6,11,12]. The reactants were pumped through a liquid N_2 trap by a mechanical pump, which maintained a pressure of 0.60 Torr with a carrier gas flow of 100 sccm into the reactor. The carrier gas was ultrahigh purity nitrogen (Airgas), which helped transport reactants into the reactor and remove reaction products from the reactor.

The in-situ FTIR studies were performed with a Nicolet Nexus 870 FTIR spectrometer equipped with a liquid-N_2 cooled mercury-cadmium-telluride (MCT-B) infrared detector. Spectra were collected with a mirror speed of $1.8\,cm \cdot s^{-1}$, and averaged over 100 scans using $4\,cm^{-1}$ resolution. The IR transparent windows on the viscous flow MLD reactor were KBr disks supplied by International Crystal Laboratories. The spectrometer setup was purged with dry and CO_2-free air delivered from a purge gas generator.

The transmission FTIR spectroscopy measurements required high surface area samples to obtain a sufficient signal-to-noise to monitor the surface species. The high surface area samples were approximately spherical nanoparticles with average diameters of 25 nm for ZrO_2 and 11 nm for SiO_2. The nanoparticles were pressed into a stainless steel grid using methods described earlier [7,35]. The stainless steel grids supporting the ZrO_2 or SiO_2 nanoparticles were obtained from Tech Etch. The ZrO_2 and SiO_2 nanoparticles were obtained from Sigma-Aldrich.

The zincone MLD growth was monitored at 90, 110, 130, 150, and 170 °C. Each DEZ exposure consisted of two 1.0 s doses of DEZ. Each DEZ dose produced a partial pressure of 200 mTorr. Each EG exposure consisted of five 1.0 s doses of EG. Each EG dose produced a partial pressure of 20 mTorr. Purge time of 120 s were used after each DEZ and EG dose. One set of DEZ and EG exposures defined one MLD cycle. The DEZ and EG reactants were obtained from Sigma-Aldrich.

The in-situ QCM measurement technique has been described previously [36]. The QCM measurements were performed in a larger viscous flow reactor using a TM-400 (Maxtek) thin film deposition monitor [6]. These measurements employed a Maxtek BSH-150 bakeable sensor, and a quartz crystal with a polished Au face and a 6 MHz oscillation frequency (Colorado Crystal Corp.).

Ex-situ XRR data were acquired by a high resolution Bede D1 Diffractometer (Bede Scientific). A Cu Kα X-ray tube with a wavelength of 1.54 Å, a filament current of 40 mA, and a voltage of 40 kV were used for the XRR measurements. The thicknesses of the zincone films on Si wafers were extracted using the REFS data fitting software from Bede Scientific. Boron doped p-type silicon wafers with a thin native oxide (Silicon Valley Microelectronics, Inc.) were used for this ex-situ analysis.

XPS images for C 1s, O 1s, and Zn 2p were obtained from a Perkin-Elmer 5600 photoelectron spectrometer with monochromatic Kα source (12.5 mA, 12 kV) under a pressure of 2×10^{-10} Torr. The binding energies were referenced to the adventitious C 1s peak at 285 eV. The TEM analysis was performed using a Philips CM10 transmission electron microscope with an 80 kV beam energy. The zincone MLD growth per cycle was determined by measuring the film thickness of the zincone polymer on the ZrO_2 nanoparticles and dividing by the number of MLD cycles.

Received: October 22, 2008
Revised: March 02, 2009

[1] S. M. George, B. Yoon, A. A. Dameron, *Acc. Chem. Res.* **2009**, *42*, 498.
[2] T. Yoshimura, S. Tatsuura, W. Sotoyama, *Appl. Phys. Lett.* **1991**, *59*, 482.
[3] S. M. George, A. W. Ott, J. W. Klaus, *J. Phys. Chem.* **1996**, *100*, 13121.
[4] M. Ritala, M. Leskela, Atomic Layer Deposition, in *Handbook of Thin Film Materials*, Vol. 1 (Ed: H. S. Nalwa), Academic Press, San Diego, CA 2002.
[5] T. Suntola, *Thin Solid Films* **1992**, *216*, 84.
[6] A. A. Dameron, D. Saghete, B. B. Burton, S. D. Davidson, A. S. Cavanagh, J. A. Bertand, S. M. George, *Chem. Mater.* **2008**, *20*, 3315.
[7] J. D. Ferguson, A. W. Weimer, S. M. George, *Thin Solid Films* **2000**, *371*, 95.
[8] M. D. Groner, J. W. Elam, F. H. Fabreguette, S. M. George, *Thin Solid Films* **2002**, *413*, 186.
[9] M. Ritala, M. Leskela, J. P. Dekker, C. Mutsaers, P. J. Soininen, J. Skarp, *Chem. Vap. Deposition* **1999**, *5*, 7.
[10] J. W. Elam, D. Routkevitch, P. P. Mardilovich, S. M. George, *Chem. Mater.* **2003**, *15*, 3507.
[11] Y. Du, S. M. George, *J. Phys. Chem. C.* **2007**, *111*, 8509.
[12] N. M. Adamcyzk, A. A. Dameron, S. M. George, *Langmuir* **2008**, *24*, 2081.
[13] M. Putkonen, J. Harjuoja, T. Sajavaara, L. Niinisto, *J. Mater. Chem.* **2006**, *17*, 664.
[14] T. Yoshimura, S. Tatsuura, W. Sotoyama, A. Matsuura, T. Hayano, *Appl. Phys. Lett.* **1992**, *60*, 268.
[15] H. I. Shao, S. Umemoto, T. Kikutani, N. Okui, *Polymer* **1997**, *38*, 459.
[16] A. Kim, M. A. Filler, S. Kim, S. F. Bent, *J. Am. Chem. Soc.* **2005**, *127*, 6123.
[17] A. Kubono, N. Okui, *Prog. Polym. Sci.* **1994**, *19*, 389.
[18] C. N. McMahon, L. Alemany, R. L. Callender, S. G. Bott, A. R. Barron, *Chem. Mater.* **1999**, *11*, 3181.
[19] B. B. Burton, F. H. Fabreguette, S. M. George, *Thin Solid Films* **2009**, (In Press).
[20] B. B. Burton, D. N. Goldstein, S. M. George, *J. Phys. Chem. C.* **2009**, *113*, 1939.
[21] O. Nilsen, H. Fjellvag, Patent Cooperation Treaty (PCT), World Intellectual Property Organization, Publication Number WO 2006/071126 A1, Publication Date July 6, 2006, Title: Thin Films Prepared with Gas Phase Deposition Technique.
[22] We initially reported our results on zincone and alucone MLD using alkyl metals and various organic diols at the AVS Topical Conference on Atomic Layer Deposition (ALD2008) in Bruges, Belgium, June 28–July 2, 2008 (B. Yoon, J.L. O'Patchen, S.D. Davidson, D. Segehte, A.S. Cavanagh, S.M. George, Molecular Layer Deposition of Hybrid Organic-Inorganic Polymers Based on Metal Alkyl and Diol Reactants, July 2, 2008).
[23] Zinc hybrid material from DEZ and EG was also reported at the AVS Topical Conference on Atomic Layer Deposition (ALD2008) in Bruges, Belgium, June 28–July 2, 2008 (Q. Peng, R.M. Vangundy, G.N. Parsons, Atomic Layer Deposition of Zinc Oxide/Organic Hybrid Material from Diethyl Zinc and Ethylene Glycol, July 2, 2008).
[24] J. W. Elam, Z. A. Sechrist, S. M. George, *Thin Solid Films* **2002**, *414*, 43.
[25] J. D. Ferguson, A. W. Weimer, S. M. George, *J. Vac. Sci. Technol. A* **2005**, *23*, 118.
[26] B. S. Sang, A. Yamada, M. Konagai, *Jpn. J. Appl. Phys. Part 2* **1998**, *37*, L206.

[27] HSC Chemistry 5.1, Outokumpu Research Oy, Pori, Finland.

[28] L. A. Schechtman, J. J. Kemper, Patent Cooperation Treaty (PCT), World Intellectual Property Organization, Publication Number WO/2000/077072, Publication Date December 21, 2000, Title: Soluble Polyfunctional Initiators for Lactone Ring-Opening Polymerization.

[29] G. Socrates, *Infrared Characteristic Group Frequencies*, Second Edition, John Wiley & Sons, Inc., New York 1994.

[30] S. D. Bunge, J. M. Lance, J. A. Bertke, *Organometallics* **2007**, *26*, 6320.

[31] Y. J. Kwon, K. H. Kim, C. S. Lim, K. B. Shim, *J. Ceram. Process. Res.* **2002**, *3*, 146.

[32] K. Maejima, S. Fujita, *J. Cryst. Growth* **2006**, *293*, 305.

[33] A. I. Rudenko, A. N. Gershuni, L. V. Kalabina, *J. Eng. Phys. Thermophys.* **1997**, *70*, 799.

[34] J. Soria, J. Sanz, I. Sobrados, J. M. Coronado, A. J. Maira, M. D. Hernndez-Alonso, F. Fresno, *J. Phys. Chem. C* **2007**, *111*, 10590.

[35] T. H. Ballinger, J. C. S. Wong, J. T. Yates, *Langmuir* **1992**, *8*, 1676.

[36] J. W. Elam, M. D. Groner, S. M. George, *Rev. Sci. Instrum.* **2002**, *73*, 2981.

